Sundarasetty, B.S., Singh, V.K., Salguero, G., Geffers, R., Rickmann, M., MacKe, L., Borchers, S., Figueiredo, C., Schambach, A., Gullberg, U., Provasi, E., Bonini, C., Ganser, A., Woelfel, T., Stripecke, R. Lentivirus-induced dendritic cells for immunization against high-risk WT1+ acute myeloid leukemia (2013) Human Gene Therapy, 24 (2), pp. 220-237.

HUMAN GENE THERAPY 24:220–237 (February 2013)

DOI: 10.1089/hum.2012.128

Lentivirus-Induced Dendritic Cells for Immunization Against High-Risk WT1$^+$ Acute Myeloid Leukemia

Bala Sai Sundarasetty,[1] Vijay Kumar Singh,[2] Gustavo Salguero,[1] Robert Geffers,[3] Mareike Rickmann,[1] Laura Macke,[1] Sylvia Borchers,[1] Constanca Figueiredo,[4] Axel Schambach,[5] Urban Gullberg,[6] Elena Provasi,[7] Chiara Bonini,[7] Arnold Ganser,[1] Thomas Woelfel,[2] and Renata Stripecke[1]

Abstract

Wilms' tumor 1 antigen (WT1) is overexpressed in acute myeloid leukemia (AML), a high-risk neoplasm warranting development of novel immunotherapeutic approaches. Unfortunately, clinical immunotherapeutic use of WT1 peptides against AML has been inconclusive. With the rationale of stimulating multiantigenic responses against WT1, we genetically programmed long-lasting dendritic cells capable of producing and processing endogenous WT1 epitopes. A tricistronic lentiviral vector co-expressing a truncated form of WT1 (lacking the DNA-binding domain), granulocyte-macrophage colony-stimulating factor (GM-CSF), and interleukin-4 (IL-4) was used to transduce human monocytes *ex vivo*. Overnight transduction induced self-differentiation of monocytes into immunophenotypically stable "SmartDC/tWT1" (GM-CSF$^+$, IL-4$^+$, tWT1$^+$, IL-6$^+$, IL-8$^+$, TNF-α^+, MCP-1$^+$, HLA-DR$^+$, CD86$^+$, CCR2$^+$, CCR5$^+$) that were viable for 3 weeks *in vitro*. SmartDC/tWT1 were produced with peripheral blood mononuclear cells (PBMC) obtained from an FLT3-ITD$^+$ AML patient and surplus material from a donor lymphocyte infusion (DLI) and used to expand CD8$^+$ T cells *in vitro.* Expanded cytotoxic T lymphocytes (CTLs) showed antigen-specific reactivity against WT1 and against WT1$^+$ leukemia cells. SmartDC/tWT1 injected s.c. into Nod.Rag1$^{-/-}$.IL2rγc$^{-/-}$ mice were viable *in vivo* for more than three weeks. Migration of human T cells (huCTLs) to the immunization site was demonstrated following adoptive transfer of huCTLs into mice immunized with SmartDC/tWT1. Furthermore, SmartDC/tWT1 immunization plus adoptive transfer of T cells reactive against WT1 into mice resulted in growth arrest of a WT1$^+$ tumor. Gene array analyses of SmartDC/tWT1 demonstrated upregulation of several genes related to innate immunity. Thus, SmartDC/tWT1 can be produced in a single day of *ex vivo* gene transfer, are highly viable *in vivo*, and have great potential for use as immunotherapy against malignant transformation overexpressing WT1.

Introduction

Despite several recent achievements in the diagnostics and treatment of acute myeloid leukemia (AML) patients, the long-term event-free survival for patients at high risk remains low (Schlenk *et al.*, 2008; Bacher *et al.*, 2009; Gupta *et al.*, 2011). The FLT3-ITD$^+$ mutation occurs in approximately 30% of AML, and relapse is the most common cause of the treatment failure (Schlenk *et al.*, 2008; Bacher *et al.*, 2009). For these patients, donor lymphocyte infusions (DLI) to boost the graft versus leukemia (GVL) effects is considered the best treatment approach, but the suboptimal anti-leukemia efficacy seen in the lymphopenic hosts may contribute to the poor overall survival rates. Thus, innovative treatment approaches to provide more robust immune regeneration or DLI efficacy to patients with high-risk AML are sought (Porter, 2011).

An important requirement for autologous or donor-derived anti-leukemia responses is the generation of long-lasting cytotoxic CD8$^+$ T cells with a broad repertoire targeted selectively against antigens (over-)expressed by leukemia cells. Wilms' tumor 1 (WT1) protein is a transcription factor aberrantly overexpressed in various solid tumors and

[1]Department of Hematology, Hemostasis, Oncology and Stem Cell Transplantation; [4]Department of Transfusion Medicine; and [5]Institute of Experimental Hematology; Hannover Medical School, 30625 Hannover, Germany.
[2]3rd Medical Department, University Medical Center of the Johannes Gutenberg University Mainz, 55101 Mainz, Germany.
[3]Genome Analytics, Helmholtz Center for Infection Research, 38124 Braunschweig, Germany.
[6]Department of Hematology, Lund University, S-221 84 Lund, Sweden.
[7]Experimental Hematology Unit, S. Raffaele Scientific Institute, 20132 Milano, Italy.

hematologic malignancies (Sugiyama, 2010). Although the intracellular pathways leading to WT1 overexpression and leukemia progression are not fully defined, WT1 expression has been explored as a prognostic marker and is a useful indicator to monitor minimal residual disease and relapse (Cilloni *et al.*, 2009). Following identification of various epitopes within the WT1 protein restricted to human leukocyte antigen (HLA) classes I and II, WT1 peptide vaccination studies were undertaken as a mode of treatment for leukemia (Rezvani *et al.*, 2008). Phase I/II clinical trials of peptide vaccination have shown that WT1-specific cytotoxic $CD8^+$ T-cell responses can be sporadically generated or enhanced in an HLA-restricted manner (Rezvani *et al.*, 2008; Keilholz *et al.*, 2009; Maslak *et al.*, 2010), but the clinical outcomes have been diverse (Kuball *et al.*, 2011; Rezvani *et al.*, 2011).

Low numbers of WT1-specific T cells with low avidity are commonly detectable in AML patients and healthy individuals (Scheibenbogen *et al.*, 2002), which may represent memory lymphocytes participating in the immune surveillance against malignancies correlated with WT1 overexpression. Therefore, several groups have explored methods to expand WT1-specific T cells by *ex vivo* culture methods or by gene transfer of transgenic T-cell receptors for adoptive immunotherapy (Ho *et al.*, 2006; Weber *et al.*, 2009; Pospori *et al.*, 2011). These methods are demanding in terms of costs and require several weeks for T-cell production. Furthermore, it remains unclear whether T cells will result in a broad repertoire of long-lasting immune surveillance. Therefore, active immunotherapy with professional antigen-presenting cells, such as dendritic cells (DC) for multi-antigenic and multivalent anti-WT1 responses remains an attractive alternative. HIV-1–derived lentiviral vectors have been broadly explored for gene delivery into hematopoietic stem cells and T cells. These quiescent primary target cells are preconditioned with homeostatic cytokines in order to stimulate the cells to progress from G0 to the G1 phase of the cell cycle, which enhances transduction efficiency (Case *et al.*, 1999; Cavalieri *et al.*, 2003). The use of lentiviral vectors for genetic modification of DC has been explored by several groups (Pincha *et al.*, 2010), but one limitation is that dendritic cells *in vivo* are usually quiescent, which may hamper lentiviral transduction. Thus, we have explored a short cytokine stimulation (8 hr) of human monocytes with granulocyte-macrophage colony-stimulating factor (GM-CSF) and interleukin (IL-4) prior to *ex vivo* lentiviral vector transduction (Koya *et al.*, 2004). We have shown that simultaneous lentiviral co-expression of GM-CSF, IL-4, and antigens in monocytes results in long-lasting "self-differentiated *m*yeloid-derived *a*ntigen-presenting cells *r*eactive against *t*umors" (SmartDC) (Salguero *et al.*, 2011; Pincha *et al.*, 2012).

Mouse SmartDC produced with bone-marrow precursors and injected subcutaneously into mice were highly viable, migrated effectively to lymph nodes, and generated potent protective and therapeutic immune responses against melanoma (Koya *et al.*, 2007; Pincha *et al.*, 2011). We successfully produced SmartDC expressing the TRP2 melanoma antigen through lentiviral gene transfer of human monocytes. We accomplished this under good manufacturing practices (GMP), which is of interest for future clinical development (Pincha *et al.*, 2012).

In this current study, we tested if a truncated form of *WT1* (lacking the DNA-binding domain; *tWT1*), along with GM-CSF and IL-4, could induce SmartDC self-differentiation and $WT1^+$-specific immune responses. SmartDC/tWT1 generated from monocytes from a $FLT3\text{-}ITD^+$ AML patient or from the related matched donor efficiently stimulated expansion and activation of anti-WT1 cytotoxic responses against primary blasts obtained from the patient. Preclinical validation studies in a 21-day xenograft huCTL NOD.$Rag1^{-/-}$.IL2r$\gamma c^{-/-}$ mouse model confirmed the high viability of SmartDC/tWT1 *in vivo* to attract CTLs. In combination with human CTLs expanded *ex vivo*, SmartDC/tWT1 inhibited $WT1^+$ tumor growth.

Materials and Methods

Design and production of lentiviral vectors

The self-inactivating (SIN) lentiviral backbone vector pRRL-sin-cPPT-hCMV-MCS-oPRE (containing a mutated nonencoding PRE) and the bicistronic vector (LV-G24) co-expressing GM-CSF and IL-4, interspaced with a porcine teschovirus-1 2A element (P2A), were previously described (Salguero *et al.*, 2011). LV expressing the truncated form of human WT1 (tWT1) was constructed with a cDNA previously characterized in transduction of CD34 cells (Svensson *et al.*, 2005). The tricistronic LV expressing GMCSF-P2A-IL-4-F2A-tWT1 (LV-G242W) was constructed by overlapping polymerase chain reaction (PCR) using LV-GM-CSF-P2A-IL-4 and LV-tWT1 as templates as previously described (Pincha *et al.*, 2012) (see Supplementary Material, available online at www.liebertonline.com/hum). Large-scale production, concentration, and titering of lentiviral constructs was described (Stripecke, 2009).

Western blot analyses

1×10^5 293T cells were transduced with LVs at a concentration of 1 μg p24/mL (1×10^7 infective viral particles/mL). After transduction, supernatants and cell pellets were collected and analyzed by Western blot and enzyme-linked immunosorbent assay (ELISA) as described in the Supplementary Material.

Peripheral blood mononuclear cells from healthy donors and AML patients

Collection of peripheral blood and leukapheresis were performed after approval by the ethics committee of the Hannover Medical School and after participants gave written informed consent. Peripheral blood mononuclear cells (PBMCs) from healthy donors and AML patients were isolated from the peripheral blood using Ficoll gradient separation and cryopreserved (Pincha *et al.*, 2012).

Generation of SmartDC or conventional DC

SmartDC were generated using an established protocol (Salguero *et al.*, 2011; Pincha *et al.*, 2012) (see also Supplementary Material). Viability *in vitro* was determined by trypan blue exclusion.

Analyses of lentiviral integration in SmartDC

Total genomic DNA was extracted from SmartDC on days 7, 14, and 21 after transduction using the QiaAmp DNA blood mini kit (Qiagen) according to the manufacturer's

instructions. Quantitative real-time PCR was performed using the Ultrarapid lentiviral titer kit according to the manufacturer's instructions (System Biosciences, BioCat GmbH). The reaction was set up according to the protocol provided with the kit. Briefly, 300 ng/2 μl of genomic DNA prepared from the above step was added to 23 μl of RQ-PCR mix containing 12.5 μl of SYBRTaq Mix with 1 μl of primer mix for WPRE or G3PDH, adjusting the volume to 23 μl with PCR grade, nuclease free water. RQ-PCR reaction was run as follows: 50°C for 2 min (1 cycle), 95°C for 10 min (1 cycle), followed by 95°C for 10 sec and 68°C for 1 min (40 cycles). Calibration curve was obtained using the standards for WPRE (provided with the kit) and G3PDH housekeeping gene (forward: 5'ACCACAGTCCATGCCATCAC and reverse: 5'TCCACCACCCTGTTGCTGTA), and the number of LV integrations was calculated.

Analyses of human GM-CSF and IL-4 transgene expression

Secreted human GM-CSF and IL-4 collected from supernatants of transduced 293T cells and SmartDC were detected as described (Salguero *et al.,* 2011; Pincha *et al.,* 2012) (see also Supplementary Material).

Analyses of WT1 expression

For immunohistochemistry analysis of WT1 expression, cytospins of 293T cells were stained with a mouse monoclonal antibody against WT1 (Biotest), followed by alkaline phosphate detection (mouse Dako REAL™ Detection System, Dako) (see also Supplementary Material). For RT-Q-PCR analysis of WT1 mRNA expression in DC, RNA was purified using a QIAmp RNeasy Minikit (QIAGEN GmbH). WT1 RNA quantification was performed according to the kit's manufacturer's instructions (WT1 ProfileQuant® Kit [ELN*]) (see also Supplementary Material). WT1 transgene expression in primary AML cells, 293T, and KA2 cells was analyzed by intracellular staining and fluorescence-activated cell sorter (FACS) analyses (see Supplementary Material).

Flow cytometry analysis of DC

Conventional or SmartDC were stained essentially as described (Salguero *et al.,* 2011; Pincha *et al.,* 2012) (see also Supplementary Material).

Stimulation of WT1-reactive T cells in vitro *in bulk cultures, thymidine incorporation, and IFN-γ ELISPOT analyses*

PBMCs were thawed and $CD8^+$ cells were enriched by MACS following manufacturer's protocol (Miltenyi Biotec). 1×10^6 $CD8^+$ T cells were co-cultured with day-7 SmartDC (alone, pulsed with WT1 peptides, or co-expressing WT1) in 10:1 ratio in a 48-well plate. Peptides used in stimulation were $WT1_{126–134}$ epitope (RMFPNAPYL, also called "RMF," an immunodominant epitope restricted to HLA*A201) or WT1 overlapping peptide mix (pepmix, all peptides from JPT Peptide Technologies). IL-2 (25 IU/mL) (Proleukin), IL-7 (5 ng/mL), and IL-15 (5 ng/mL) (Cellgenix) cytokines were added to the culture every 2 days during the stimulation. Ten days after the stimulation, restimulation was performed in a similar culture condition. After each stimulation, T-cell numbers were determined for further stimulation analyses and a total of three stimulations were performed. Thymidine incorporation was performed essentially as described (Pincha *et al.,* 2012) (see also Supplementary Material).

Stimulation of WT1-reactive T cells in vitro *in microcultures and IFN-γ ELISPOT after incubation with KA2 target cells*

Microcultures for T-cell stimulation and ELISPOT were performed as described (Pincha *et al.,* 2012) (see also Supplementary Material).

Streptamer analyses

The frequency of T cells harboring the TCR reactive against the $WT1_{126–134}$ epitope was analyzed with Strep-Tactin phycoerythrin (PE) conjugated MHC class I multimers specific for $WT1_{126–134}$ (RMFPNAPYL) streptamer (IBA GmbH). Staining was performed according to the manufacturer's protocol (see also Supplementary Material).

Carboxyfluorescein diacetate succinimidyl ester (CFSE)-based cytotoxicity analyses

Carboxyfluorescein diacetate succinimidyl ester (CFSE)-based cytotoxicity analyses were performed in a 96-well plate as described (Jedema *et al.,* 2004) (see also Supplementary Material).

CD107a degranulation assay

CD107a is a marker for the cytolytic activity of T cells after stimulation with target cells (Betts *et al.,* 2003). $CD8^+$ T cells expanded with SmartDC were harvested and co-cultured with CFSE-labeled primary AML cells at various effector-to-target ratios. APC-anti-CD107a (Biolegend GmbH) was added to the co-cultures and incubated at 37°C and 5% CO_2 for 4 hours. After the incubation, T cells were stained with PE/Cy7-anti-CD8 (BD Biosciences) and PE/Texas Red- anti-CD3 (Beckman Coulter). $CFSE^-/CD3^+/CD8^+$ T cells were gated and the frequency of the CD107a positive cytotoxic population was obtained.

Stimulation of WT1-reactive T cells in vivo *using a KA2/tWT1 murine adoptive T-cell transfer model*

All procedures involving mice were reviewed and approved by the Lower Saxony State Office for Consumer Protection and Food Safety and followed the guidelines provided by the Animal Facility at the Hannover Medical School. NOD.Cg-*Rag1*^{tm1Mom} *Il2rg*^{tm1Wjl} (Nod.Rag1$^{-/-}$.IL2rγc$^{-/-}$, NRG) mice were bred in house and maintained under pathogen-free conditions in an IVC system (BioZone). SmartDC/tWT1 viability *in vivo* and T-cell biodistribution analyses in NRG mice were followed by optical imaging analyses as previously described (Salguero *et al.,* 2011). For tumor inhibition studies, cell suspensions containing SmartDC/tWT1 vaccine (left side) and KA2/tWT1 tumor transduced with LV-fLUC (right side) were subcutaneously injected at a dose of 5×10^5 cells in 100 μL of PBS into NRG mice hind flank using a 27-gauge needle. Seven days later, T-cell suspensions (2×10^6 cells in 100 μL of PBS) were injected into the lateral tail vein. At different time points, growth of KA2/tWT1/fLUC was evaluated by *in vivo* bioluminescence imaging analyses.

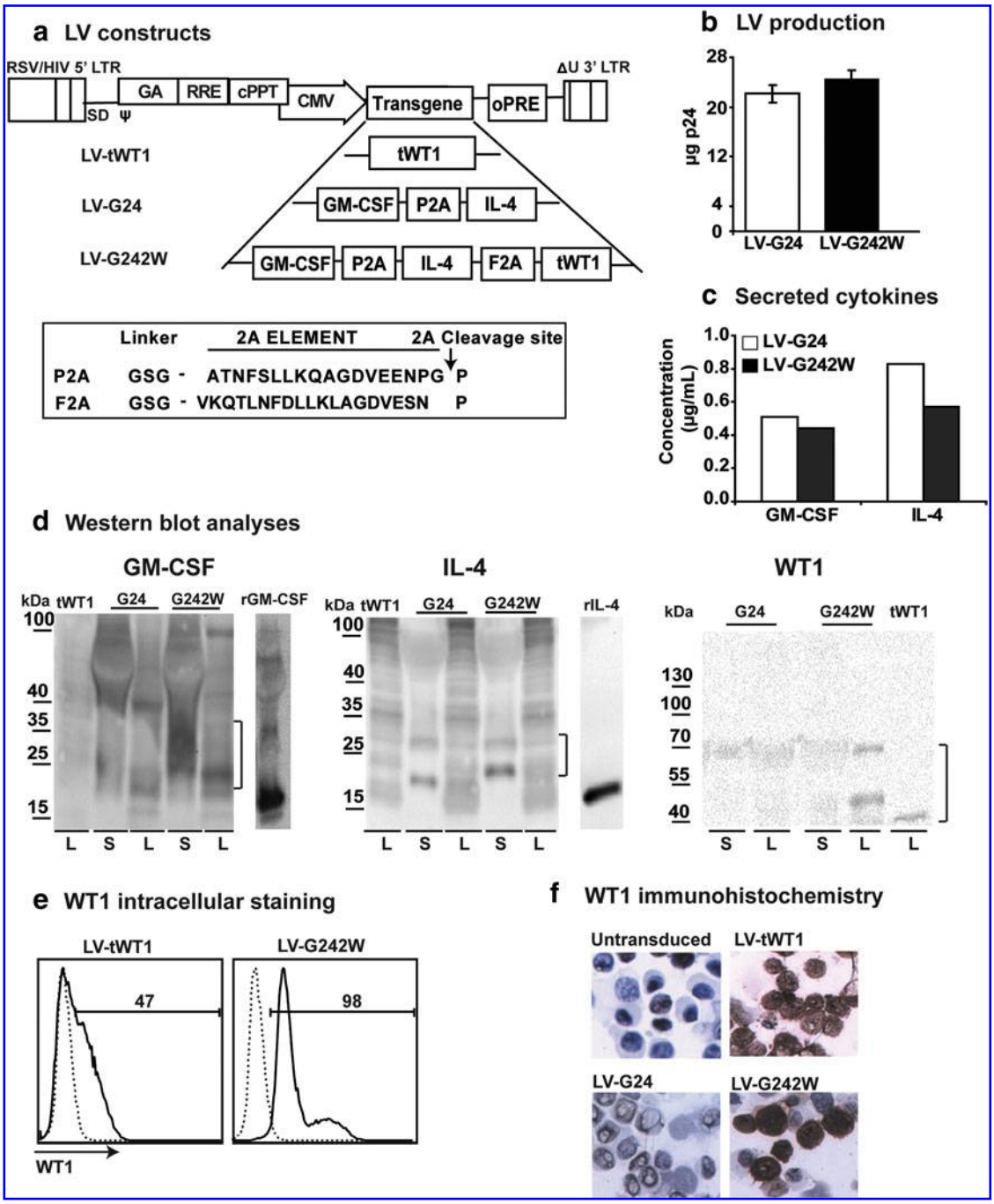

FIG. 1. Lentiviral vectors (LV) and characterization of transgene expression: Vector constructs, titers, and western blot analyses. **(a)** Schematic representation of monocistronic LV-expressing truncated form of Wilms' Tumor 1 (tWT1) and bicistronic vector (LV-G24) co-expressing granulocyte-macrophage colony stimulating factor (GM-CSF) and interleukin-4 (IL-4), interspaced with a 2A element derived from porcine teschovirus (P2A) and tricistronic vector co-expressing GM-CSF, IL-4, and tWT1, interspaced by two 2A elements; P2A and another 2A element derived from foot-and-mouth virus (F2A). The amino acid sequences of 2A elements are shown with the peptide cleavage site indicated by an arrow. **(b)** The total yield of virus productions (six independent runs) for the bi- and tricistronic vectors quantified by p24 detection. Error bars indicate standard error of mean (SEM). **(c)** Accumulated levels of human GM-CSF and IL-4 in transduced 293T-cell supernatants determined by enzyme-linked immunosorbent assay (ELISA). **(d)** Western blot analyses of GM-CSF, IL-4, and tWT1 from the supernatants (S) and lysates (L), obtained from 293T cells transduced with LV-WT1, LV-G24, and LV-G242W. The parentheses indicate the transgenic proteins on the blot. Recombinant GM-CSF and IL-4 were used as reference controls. **(e)** Flow cytometry analyses of intracellular WT1 expression in 293T cells transduced with LV-WT1 and LV-G242W. **(f)** Immunohistochemistry analyses of transduced 293T cells with LV-WT1, LV-G24, and LV-G242W. Darker stained cells indicate the expression level of WT1 in cells, whereas the light grey color indicates lack of expression. Nontransduced 293T cells were used as negative controls. Color images available online at www.liebertpub.com/hum

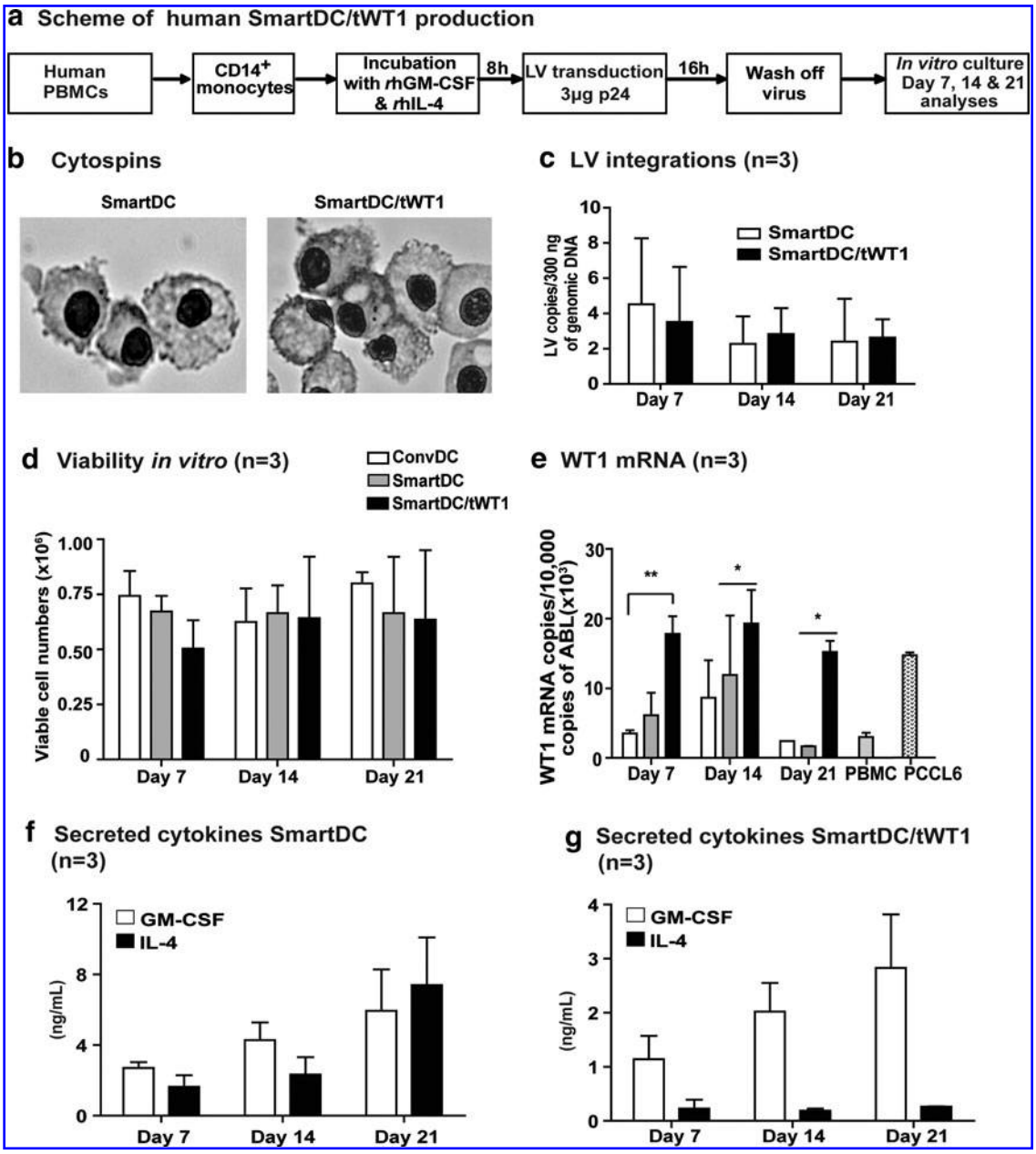

FIG. 2. Production of dendritic cells programmed with lentiviral vectors. **(a)** Schematic representation of SmartDC generation from human peripheral blood mononuclear cells (PBMCs). **(b)** Cytospin analyses (day 7) showing the typical DC morphology in SmartDC and SmartDC/tWT1. Both groups show dendrites on the cell surface, typical of DC. **(c)** Monocytes transduced with LVG24 and LVG242W and the number of integrated LV copies was quantified by quantitative polymerase chain reaction (qPCR) 7, 14, and 21 days post transduction. Histogram bars represent the data obtained from experiments performed with cells from three different donors (n = 3) and LV integrations are expressed as the number of LV copies per 300 ng of genomic DNA. **(d)** Viable cell counts of SmartDC/tWT1 after days 7, 14, and 21 in comparison to ConvDC and SmartDC. **(e)** Expression of WT1 (mRNA) in DC on days 7, 14, and 21. Histogram bars represent the normalized values of WT1 against ABL. PBMCs from healthy donors are used as negative control, and PCCL6 is the positive control. Error bars indicate the average and SEM. $*p < 0.05$ and $**p < 0.01$. **(f)** Transgenic GM-CSF and transgenic IL-4 (secreted) from SmartDC and **(g)** transgenic GM-CSF and transgenic IL-4 (secreted) from SmartDC/tWT1 analyzed from the supernatants obtained from DC cultures at days 7, 14, and 21. Histogram bars represent average levels of cytokines determined in triplicate experiments with three independent donors (n = 3).

Microarray analyses

RNA was extracted from the cells using RNeasy mini kit (Qiagen). Quality and integrity of the total RNA was controlled on an Agilent Technologies 2100 Bioanalyzer (Agilent Technologies). Five hundred ng of total RNA were applied for Cy3-labelling reaction using the one-color Quick Amp Labeling protocol (Agilent Technologies). Labeled cRNA was hybridized to Agilent's human 4x44k microarrays for 16 hr at 68°C and scanned using the Agilent DNA Microarray

Scanner. Expression values were calculated by the software package Feature Extraction 10.5.1.1 (Agilent Technologies). (See also Supplementary Material).

Statistical Analysis

Student's t-tests and Bonferroni post-tests were performed for the data derived using the GraphPad Prism software. All tests were two-sided and the p-values < 0.05 were considered significant and were duly indicated.

Results

LV-G242W: a tricistronic LV co-expressing GM-CSF, IL-4, and truncated WT1

We have previously demonstrated that multicistronic LVs co-expressing GM-CSF and IL-4 induced direct self-differentiation of human and murine DC precursors into highly viable and potent SmartDC (Koya *et al.*, 2007; Pincha *et al.*, 2011, 2012; Salguero *et al.*, 2011). In this study, we designed a tricistronic vector LV-G242W co-expressing GM-CSF, IL-4, and truncated WT1 (tWT1) using interspacing 2A elements (Fig. 1a). 2A elements were used to obtain efficient translation of the three protein products at similar levels from a single open-reading frame. Two different 2A elements were used (porcine teschovirus [P2A] and foot and mouth disease virus [F2A]) in order to avoid homologous recombination in the LV (Fig. 1a). As a control, we also generated a monocistronic LV expressing tWT1. Bi- and tricistronic vectors were consistently produced at high titers (average 25 μg of p24 equivalent per production run) (Fig. 1b). Initial validation of the tricistronic LV construct LV-G242W was performed with transduced human embryonic kidney 293T cells. 293T cells transduced with LV-G24 and LV-G242W secreted high levels of GM-CSF (LV-G24: 0.5 μg/mL; LV-G242W: 0.4 μg/mL) and IL-4 (LV-G24: 0.8 μg/mL; LV-G242W: 0.5 μg/mL) (Fig. 1c). The co-expression of the individual protein products at the molecular level was characterized by Western blot analyses using protein extracts prepared with cell supernatants and cell lysates. GM-CSF and IL-4 were detectable in supernatant and lysate fractions whereas tWT1 accumulated in the cell lysates. The higher molecular weights of GM-CSF and IL-4 expressed by the tricistronic vector compared to the recombinant cytokines reflect the addition of the 2A elements and glycosylation (Fig. 1d). Expression of tWT1 in 293T cells transduced with LV-tWT1 and LV-G242W was also characterized by intracellular staining followed by flow cytometry (Fig. 1e) and by immunohistochemistry analyses (Fig. 1e). Truncated WT1 lacking the DNA-binding domain was distributed evenly in the nucleus and cytoplasm of transduced 293T cells (Fig. 1f).

Feasibility of SmartDC/tWT1 production with LV-G242W-transduced monocytes

We next evaluated whether co-expression of tWT1 mediated by the tricistronic vector in transduced monocytes affected their differentiation into viable SmartDC/tWT1. Conventional DC (ConvDC) maintained continuously in the presence of recombinant cytokines and our standard SmartDC produced with a bicistronic LV served as controls. Monocytes obtained from three different healthy donors were used to generate SmartDC using a routine protocol (Salguero *et al.*, 2011; Pincha *et al.*, 2012) (Fig. 2a). Lentivirally induced DC demonstrated typical DC morphology (Fig. 2b). Analyses of genomic DNA of SmartDC and SmartDC/tWT1 by PCR showed comparable levels of lentiviral integration for the two groups (Fig. 2c), which was associated with high viability in culture in the absence of exogenously added cytokines (Fig. 2d). Expression of tWT1 mRNA in SmartDC/tWT1 was quantified by RT-Q-PCR analyses using PBMC as negative control. Lower, but detectable, levels of WT1 mRNA copies were observed in conventional DC, SmartDC, and PBMC. SmartDC/tWT1 consistently showed significantly higher WT1 mRNA copy levels compared to the other DC groups, but comparable levels to the positive control, the leukemia cell line PCCL6 (Fig. 2e). GM-CSF and IL-4 were detectable by ELISA in continuous SmartDC culture supernatants, which increased from day 7 to day 21 (on day 21: GM-CSF: 5.95 ng/mL; IL-4: 7.4 ng/mL) (Fig. 2f). SmartDC/tWT1 also showed continuous increase of accumulated GM-CSF during the 3-week period, although lower levels than SmartDC (on day 21: 2.83 ng/mL). Remarkably, the levels of accumulated IL-4 in SmartDC/tWT1 supernatants were substantially lower (10-fold) than in SmartDC cultures, and the levels did not increase during the 3-week period (day 7: 0.18 ng/mL and day 21: 0.27 ng/mL) (Fig. 2g). This differs from the results obtained with detection of secreted cytokines in the supernatants of transduced 293T cells (Fig. 1c), which showed that the two vectors yielded comparable expression levels for GM-CSF and IL-4. Thus, the lower levels of IL-4 accumulated in supernatant cultures of SmartDC/tWT1 do not seem to result from problems in the tricistronic vector, but rather physiological changes in the DC that may be resultant from tWT1 co-expression (such as hypothetically lower secretion rates or higher autocrine cytokine utilization).

Identity and potency markers of SmartDC/tWT1

Quality control (Q/C) of cellular products is based on purity, identity, and potency markers. We had previously characterized immunophenotypic antigens and cytokines

FIG. 3. Effects of truncated form of WT1 expression in SmartDC: Identity and potency markers for SmartDC/tWT1. **(a)** Representative example of immunophenotypic marker analyses of SmartDC/tWT1 in comparison to ConvDC and SmartDC (day 7). Dotted lines indicate the isotype controls for the respective antibody staining, and the full lines indicate the relevant monoclonal antibodies. Numbers indicate the percent positive cells for the appropriate immunophenotypic marker. **(b)** Comparison of immunophenotypic identity markers in ConvDC, SmartDC, and SmartDC/tWT1—(i) HLA-DR and (ii) CD86. Histogram bars represent the data obtained from experiments performed with cells from three different donors (n = 3). **(c)** Endogenously secreted identity cytokines; GM-CSF and IL-4 and potency cytokine markers; IL-8, TNF-α, IL-6, and MCP-1 analyzed from the supernatants obtained from SmartDC and SmartDC/thWT1 cultures (day 7). Data represent the average of experiments performed with cells obtained from three different donors (n = 3). Error bars indicate SEM.

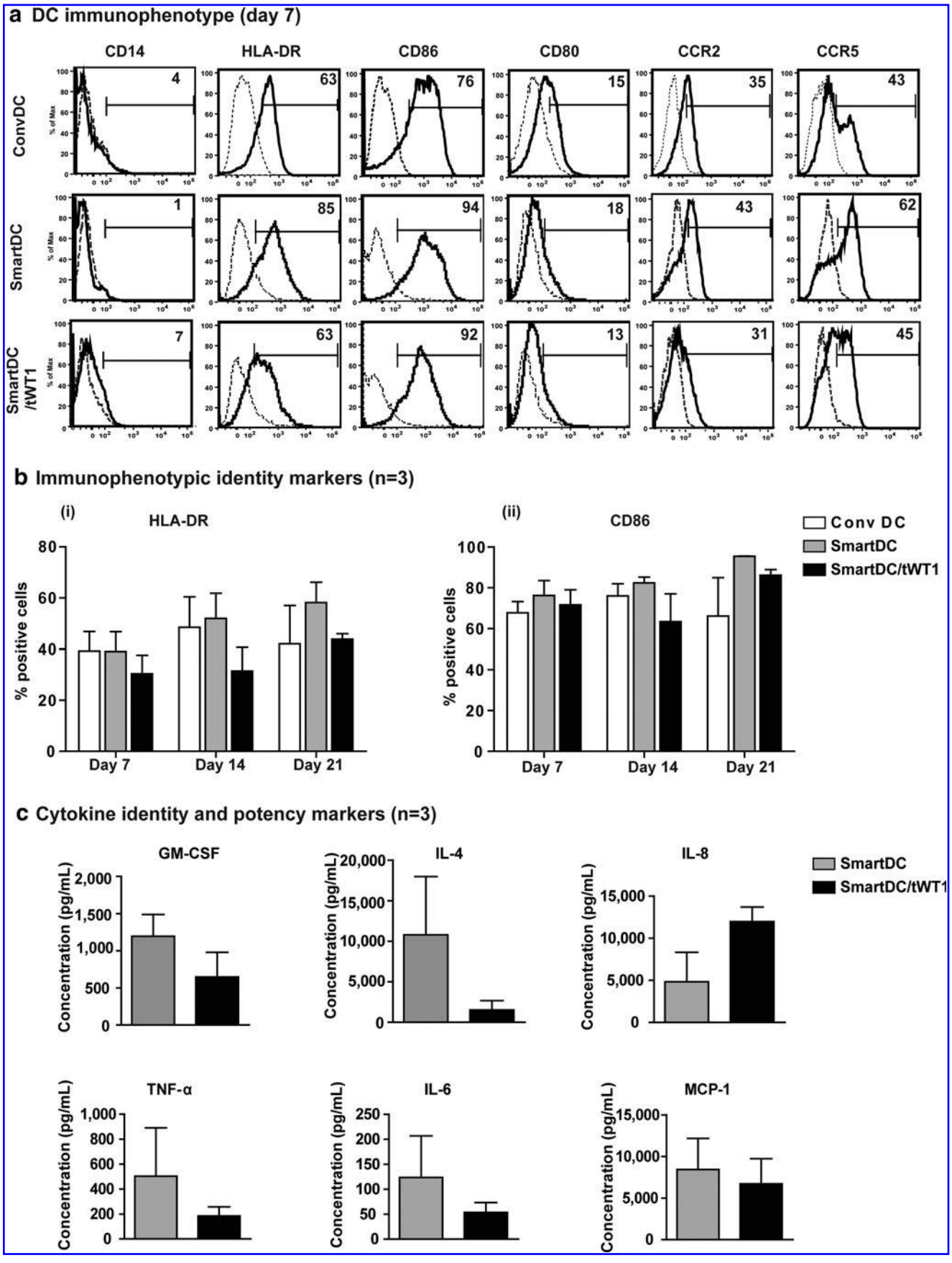
a DC immunophenotype (day 7)
CD14
HLA-DR
CD86
CD80
CCR2
CCR5
ConvDC
SmartDC
SmartDC /tWT1
% of Max
4
63
76
15
35
43
1
85
94
18
43
62
7
63
92
13
31
45
b Immunophenotypic identity markers (n=3)
(i)
HLA-DR
(ii)
CD86
% positive cells
Day 7
Day 14
Day 21
Conv DC
SmartDC
SmartDC/tWT1
c Cytokine identity and potency markers (n=3)
GM-CSF
IL-4
IL-8
TNF-α
IL-6
MCP-1
Concentration (pg/mL)
SmartDC
SmartDC/tWT1

that could serve as Q/C criteria for batch-release testing of SmartDC expressing the TRP2 melanoma antigen (Pincha *et al.*, 2012). Since tWT1 could potentially exert regulatory functions in dendritic cells and alter their differentiation, phenotypic, and functional characteristics, we examined the expression of the same immunophenotypic markers by flow cytometry. Seven days after transduction, SmartDC/tWT1 showed typical DC immunophenotype, comparable to conventional DC and SmartDC: downregulation of monocytic marker CD14 on the cell surface and upregulation of HLA-DR, CD86, CD80, CCR2, and CCR5 (Fig. 3a). Analyses of the immunologically relevant DC markers HLA-DR and CD86

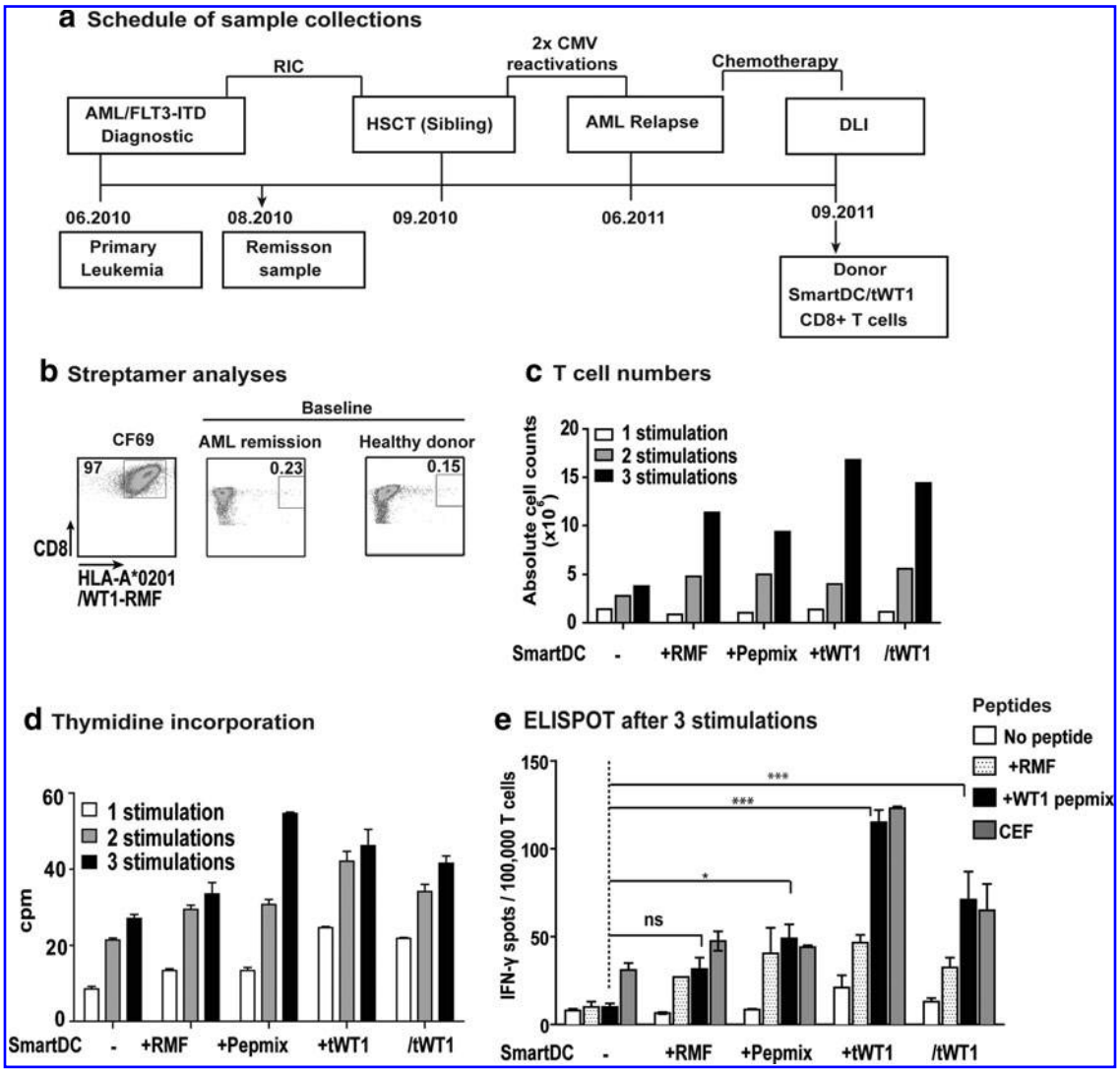

FIG. 4. Effects of SmartDC/tWT1 on $CD8^+$ T-cell expansion in bulk cultures (Healthy donor). **(a)** Schematic representation showing the collection dates of PBMCs from a FLT3-ITD^+ HLA-A*02:01^+ AML patient sample collection diagnostic and in remission after reduced intensity conditioning (RIC) chemotherapy and from the HLA-A*02:01^+ HSCT donor as a donor lymphocyte infusion (DLI) leukapheresis sample. **(b)** Baseline WT1 reactive T cells were analyzed by streptamers specific for WT1 immuno-dominant epitope: HLA-A*02:01-RMFPNAPYL ($WT1_{126–134}$). The dot plots show the frequency of $CD8^+$ T cell reactive against HLA-A*02:01-$WT1_{126–134}$ A clone (CF69) expressing the $WT1_{126–134}$ specific T-cell receptor was used as positive control, and HIV streptamer is used as nonspecific/negative control in the experiment. **(c)** Viable T-cell numbers in each stimulation group was determined by Trypan blue dye exclusion. Culture groups: SmartDC (1×10^6), SmartDC loaded with $WT1_{126–134}$ (RMF; 1×10^6), SmartDC loaded with WT1 peptide mix (1×10^6), SmartDC co-transduced with tWT1 (1×10^6), and SmartDC/tWT1 (1×10^6). Histogram bars represent absolute T-cell numbers after each stimulation cycle. **(d)** Thymidine incorporation analyses showing the proliferative capacity of $CD8^+$ T cells. $CD8^+$ T cells, after each stimulation cycle, were incubated with thymidine (^3H), and the uptake was measured by scintillation counter. The data is the representation of triplicate wells per group per stimulation. Error bars indicate mean + SEM. **(e)** ELISPOT analyses after third stimulation cycle. After three stimulations, 100,000 $CD8^+$ T cells harvested from each stimulation group were cultured in presence of no peptide, RMF peptide (HLA-A*02:01-$WT1_{126–134}$), WT1 peptide mix, and CEF for 20 hr, and the IFN-γ-secreting $CD8^+$ T cells were detected by ELISPOT. Histogram bars represent the average data from duplicate wells from each stimulation group. White bars indicate the T cells alone without any peptide, and the black bars indicate T cells with WT1 peptide mix. Error bars represent mean + SEM. Ns, not significant; $*p<0.05$; $***p<0.001$.

performed with cells produced from three different donors and at different time-points after transduction (days 7, 14, and 21) demonstrated reproducible and stable expression for all three DC groups (Fig 3b).

In addition to surface antigens, cytokines can also serve as identity and potency markers. Bead array analyses corresponding to a panel of several Th1/Th2 cytokines confirmed the presence of GM-CSF and IL-4 in culture supernatants as identity markers. Additional cytokines corresponding to endogenously upregulated potency markers were detectable, such as interleukin 8 (IL-8, a type-2 cytokine and chemokine), tumor necrosis factor α (TNF-α, a type-1 cytokine), interleukin-6 (IL-6, a Th1/Th2 cytokine), and monocyte chemotactic protein-1 (MCP-1, a chemokine) (Fig. 3c). Thus, SmartDC/tWT1 produced a mixed pattern of cytokines and chemokines, reflecting a broad homeostatic and inflammatory plasticity for activation and/or chemo-attraction of different types of cells.

SmartDC/tWT1-mediated expansion of WT1-reactive donor-derived CD8$^+$ T cells in bulk cultures

We next sought to demonstrate the effects of SmartDC/tWT1 in the stimulation of CD8$^+$ cytotoxic T cells in antigen-restricted manner. Remission samples obtained after reduced intensity conditioning (RIC) from an HLA-A*02:01 AML patient and from the stem-cell donor were analyzed by tetramer staining and showed detectable levels of CD8$^+$ T cells containing T-cell receptors reactive against the WT1$_{126–134}$ epitope (Fig. 4a and b). We used monocytes from the donor to produce SmartDC in different configurations: not loaded with antigen (-), loaded with WT1$_{126–134}$ peptide (RMF), loaded with an overlapping WT1 peptide mix (pepmix), co-transduced with a lentiviral vector expressing tWT1 (+tWT1), or transduced with the tricistronic vector (/tWT1). SmartDC cultured for seven days after transduction were used to stimulate autologous CD8$^+$ T cells at a ratio of 1:10 (1 SmartDC to 10 T cells). CD8$^+$ T-cell expansion was observed in all groups but was higher for groups stimulated with SmartDC+tWT1 or SmartDC/tWT1 expressing tWT1 endogenously (approximately 15-fold expansion after three stimulations, relative to the starting T-cell number) (Fig. 4c). T-cell expansion was further confirmed by thymidine incorporation assays (Fig. 4d). The functionality of the expanded T cells was evaluated by IFN-γ ELISPOT assay. After three rounds of stimulation, T cells were incubated with WT1$_{126–134}$ or with WT1 peptide mix and analyzed for IFN-γ production. T cells not incubated with peptides and T cells

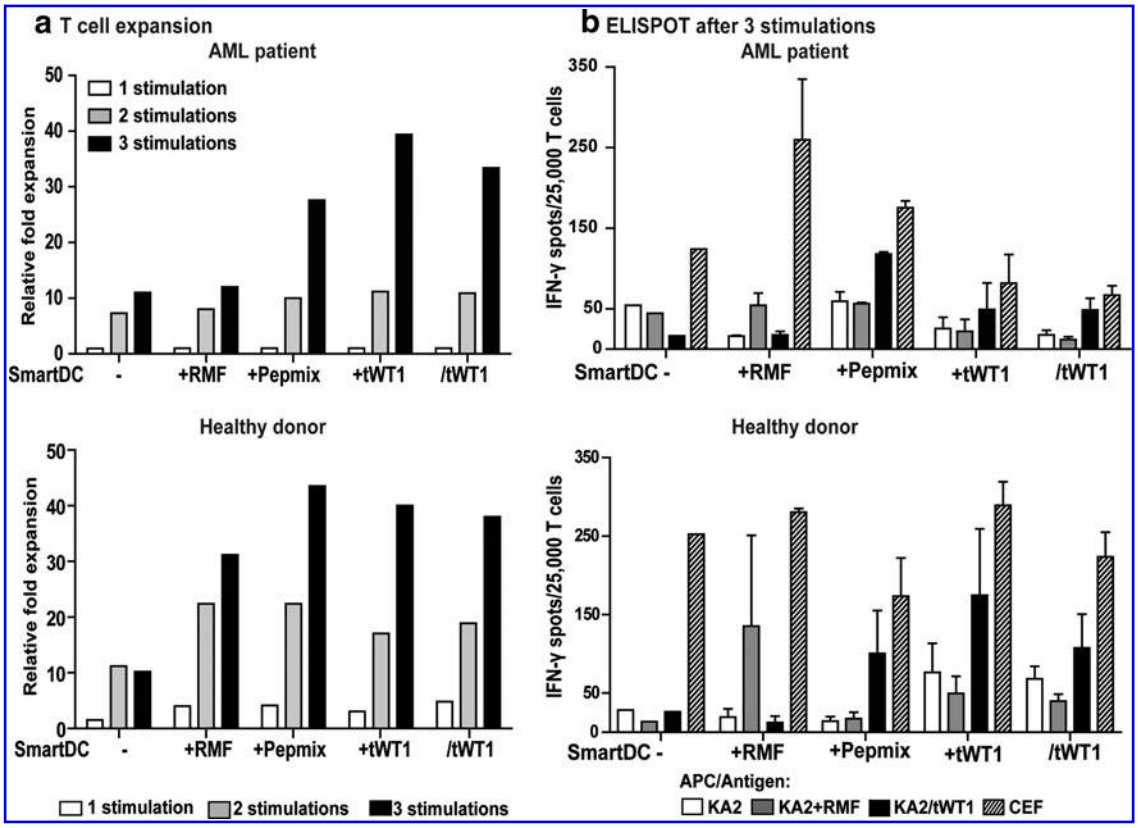

FIG. 5. Effects of SmartDC/thWT1 on antigen-specific CD8$^+$ T-cell responses in microcultures using AML patient remission samples or HLA-matched healthy donor PBMC. **(a)** T-cell expansion depicted as relative fold expansion was determined by the Trypan blue dye exclusion. Starting number of cells per microculture group: SmartDC: 2×10^5; SmartDC+RMF: 2×10^5; SmartDC+Peptidemix: 2×10^5; SmartDC+tWT1: 3×10^5; and SmartDC/tWT1: 3×10^5. Bar graphs show the relative expansion in the microculture groups after every stimulation cycle. **(b)** 25,000 CD8$^+$ T cells harvested from the respective independent microcultures after 3 stimulation cycles were used to detect their ability to secret IFN-γ in response to the target cells with or without antigen. KA2 cells are used as target cells, either alone, loaded with WT1$_{126–134}$, or expressing tWT1 endogenously. The average IFN-γ spots from duplicate wells per group were quantified after 20 hours of co-culture with targets. Bar graphs show the grouped data from independent microculture wells. White bars indicate T cells alone in each group, whereas black bars indicate T cells co-cultured with KA2/tWT1. Error bars indicate mean+SEM.

Table 1. Summary of T-cell Expansion Analyses: Results from Three Independent Runs

		Fold expansion			*ELISPOT IFN-γ spots/100,000 cells*		
Sample	*Cell source*	*SmartDC*	*SmartDC + Pepmix*	*SmartDC/ tWT1*	*SmartDC*	*SmartDC + Pepmix*	*SmartDC/ tWT1*
Healthy donor	Donor lymphocyte infusion (DLI)	10	44	38	100	402	430
AML 1 (ITD^+)	Remission	11	28	33	74	472	270
AML 2 (ITD^-)	Remission	14	23	26	23	50	117

Summary of T-cell stimulation assays performed in microcultures with PBMCs from a healthy donor and two leukemia patients (FLT3-ITD positive and negative). T-cell expansion represents the numbers of $CD8^+$ T cells detected in the culture after stimulation with SmartDC in comparison to input. Expanded $CD8^+$ T cells were evaluated for the WT1-specific immune response by IFN-γ ELISPOT assay using KA2/tWT1 cells as targets.

co-cultured with CEF recall antigens served as negative and positive controls, respectively. Higher frequencies of WT1-reactive T cells (comparable to the CEF recall control) were observed in T-cell cultures expanded with SmartDC + tWT1 and SmartDC/tWT1 compared to nonloaded SmartDC ($^*p < 0.05$; $^{***}p < 0.001$) (Fig. 4e).

SmartDC/tWT1 expansion of patient- and donor-derived $CD8^+$ T cells in microcultures and cross-reactivity against KA2/tWT1 targets

Due to the limiting amounts of PBMC obtained from patients and donors, we established microculture-based methods in order to increase the potency of the $CD8^+$ T-cell stimulation assays. The experimental scheme consisted of three rounds of T-cell stimulation in 96-well plates, so that multiple oligoclonal microcultures were obtained. In order to allow several HLA-A*02:01-restricted WT1 epitopes to be endogenously processed and presented to expanded T cells, K562 cells expressing HLA-A*02:01 (Britten *et al.,* 2002) and transduced with tWT1 (heretofore K2A/tWT1) were used (see Supplementary Fig. 2a). SmartDC, SmartDC + tWT1, and SmartDC/tWT1 generated from the patient and from the healthy donor showed normal viability and immunophenotype (Supplementary Fig. 1b), and *in vitro* culture after cryopreservation did not affect their characteristics. SmartDC loaded with WT1 peptides or co-expressing tWT1 were incubated with $CD8^+$ T cells in the presence of cytokines (IL-2, IL-7, and IL-15).

Three rounds of weekly stimulations were performed and T cells were harvested for analyses after every stimulation period. Expansion of T cells obtained from the patient and from the donor were higher after stimulation with SmartDC presenting overlapping WT1 epitopes (pepmix, +tWT1 and /tWT1, corresponding to 30- to 40-fold expansion) than with the single RMF epitope (10- to 30-fold expansion). In contrast, T-cell expansion with unloaded SmartDC reached plateau already after two stimulations (up to 10-fold expansion) (Fig. 5a). The functional capacity of these stimulated T cells to produce IFN-γ after co-culture with target KA2 cells was tested in ELISPOT assays. KA2 cells expressed a low level of endogenous WT1, but expression increased substantially following transduction with the LV-tWT1 vector (Supplementary Fig. 2a [i]). Unloaded KA2 cells, KA2 cells pulsed with peptides, or transduced for tWT1 overexpression were compared in their capability to serve as targets for cytotoxic $CD8^+$ T cells.

CEF given to the T-cell culture was used as a nonspecific stimulation control. This method resulted in detectable anti-WT1 reactivity, but notably, only when KA2 cells transduced for tWT1 expression were used as targets (Fig. 5b). KA2 cells and KA2 cells pulsed with the $WT1_{126–134}$ peptide were not efficient targets for the expanded T cells. This indicated that the anti-WT1 cytotoxic reactivity seems to be highly dependent on the level of WT1 endogenous presentation by the target cells, which is an important consideration, since hematopoietic stem and progenitor cells express lower levels of WT1 than leukemia cells (Sloand *et al.,* 2011). T-cell expansion and anti-WT1 reactivity were highly correlated for both the analyses performed with samples obtained from the healthy donor and the AML patient. Notwithstanding, superior reactivity was observed in the T cells expanded from the donor, probably indicating higher frequencies of WT1-reactive T cells that were not deleted or tolerized due to leukemia progression. Detection of T cells reactive against WT1 after stimulation with SmartDC/tWT1 was only possible after two or three stimulations (Fig. 5b; Supplementary Fig. 2b). The expansion and reactivity of the $CD8^+$ T cells was reproduced for an additional AML patient. The summary of the three independent *in vitro* expansion experiments is shown in Table 1.

Streptamer analyses of individual T-cell microcultures to evaluate the accumulation of T cells specific for $WT1_{126–134}$ by the TCR showed a correlation with the IFN-γ ELISPOT assays only for CTLs from the healthy donor (Supplementary Fig. 2c and d).

Cytotoxicity of WT1-reactive T-cell cultures

In order to correlate the IFN – γ production of the $CD8^+$ T cells expanded in the microcultures with their actual capability to lyse KA2/tWT1 targets, we performed CFSE and CD107-based cytotoxicity assays (Fig. 6a). KA2/tWT1 cells were efficiently labeled with CFSE, allowing the cells to be followed by flow cytometry analyses after mixed co-cultures with T cells (Supplementary Fig. 3a). T-cell lines obtained from the AML patient and from the healthy donor after stimulation with SmartDC/WT1 peptide mix or with SmartDC/tWT1 were compared. WT1 expression analyses in both targets (KA2/tWT1 and primary AML) were performed by intracellular staining (Fig. 6b). T-cell lines stimulated with SmartDC unloaded or loaded with the RMF single epitope showing low IFN-γ production by ELISPOT were used as controls and analyses were performed at various effector-to-target ratios

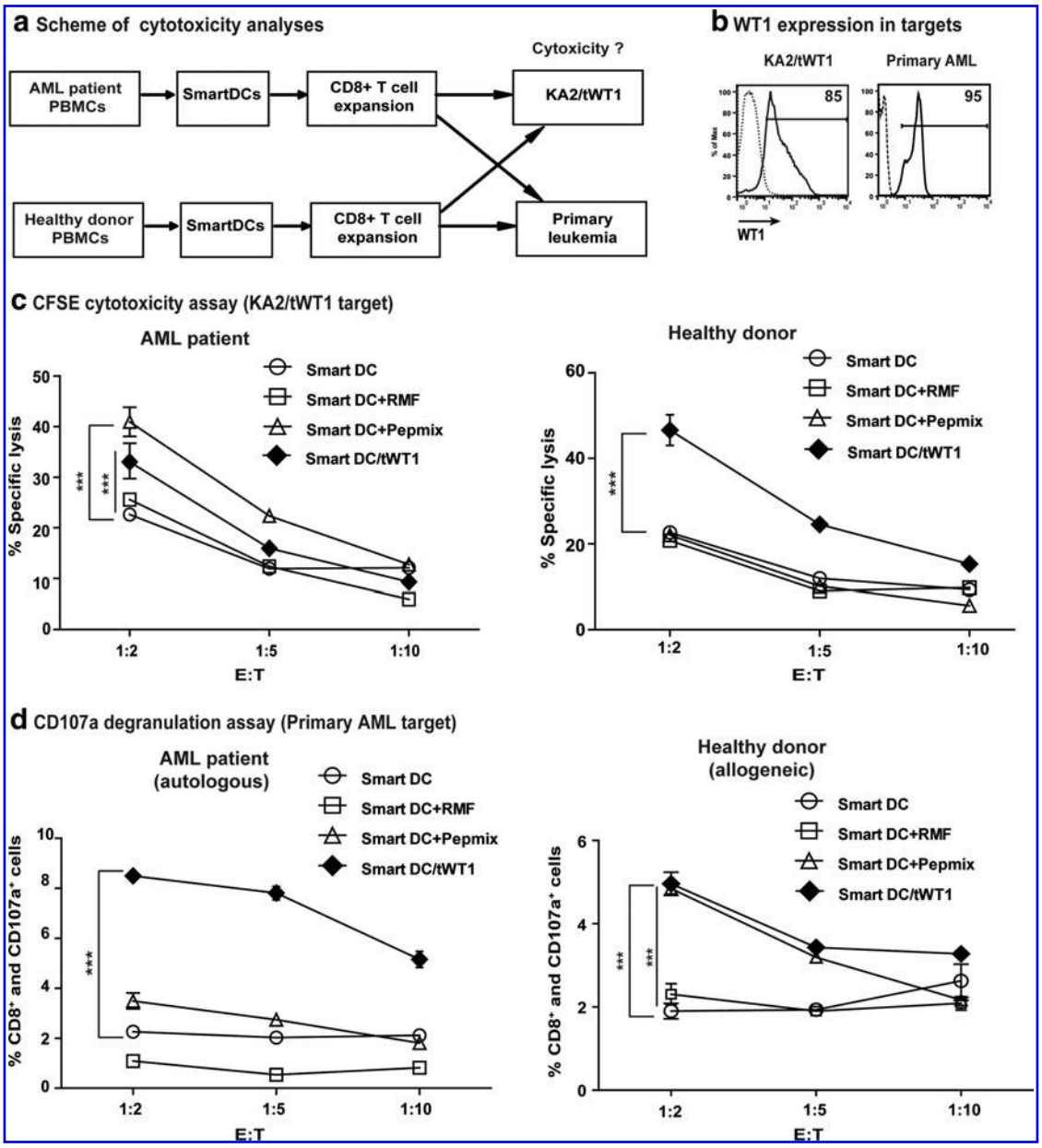

FIG. 6. Cytotoxicity analyses of WT1 reactive T cells generated from the microcultures. **(a)** Schematic representation of the cytotoxic analyses used in determining the specificity of the WT1 reactive T cells generated. A CFSE-based cytotoxicity assay and a CD107a-based degranulation assay were performed at various effector-to-target ratios after three stimulations in 96-well 'U' bottom plates. **(b)** WT1 expression in the targets cells; KA2/tWT1 and primary AML cells, analyzed by intracellular staining for WT1. Both targets, as expected, showed high levels of WT1 expression (85% and 95% respectively). **(c)** CFSE-based cytotoxicity assay. The line graph shows the percentage-specific lyses of T cells obtained from the microcultures of AML remission sample and healthy donor. The data represents the average of triplicate wells performed with cells obtained from microcultures after three stimulations and KA2 alone or KA2/tWT1 were used as targets. **(d)** The responding microcultures were thawed and analyzed for their ability to recognize the primary leukemic blasts from the AML patient in a CD107a de-granulation assay. $CD8^+$ T cells from AML patient sample were co-cultured with the AML patient's PBMCs (first diagnosis) in an autologous setting, and $CD8^+$ T cells from healthy donor were co-cultured with AML patient's PBMCs (first diagnosis) in an allogeneic setting at various effector-to-target ratios, exploring the possibility of donor-lymphocyte infusion. The cultures were simultaneously stained with CD107a monoclonal antibody conjugated with the fluorochrome, APC. The line graph shows the average data from triplicate wells of $CD8^+$ and $CD107a^+$ T cells at shown effector-to-target ratios. T cells that were stimulated with SmartDC without any antigen is shown in open circles; T cells stimulated with SmartDC/tWT1 were shown in black diamonds. Error bars indicate mean + SEM; $***p < 0.001$

(Fig. 6c). T cells generated from the AML patient after stimulation with SmartDC/WT1 peptide mix and SmartDC/tWT1 at the highest E:T ratio (1:2) resulted in significant (***$\rho < 0.001$) cytotoxicity compared with the control T cells. Notably, for the T cells generated from the healthy donor, only the T cells expanded with SmartDC/tWT1 were significantly (***$\rho < 0.001$) superior to controls (Fig. 6c). Taken together, T cells expanded with SmartDC/tWT1 from the donor were superior in HLA-A*02:01 restricted cytotoxicity than the T cells expanded with SmartDC pulsed with the WT1 peptide mix, whereas for the

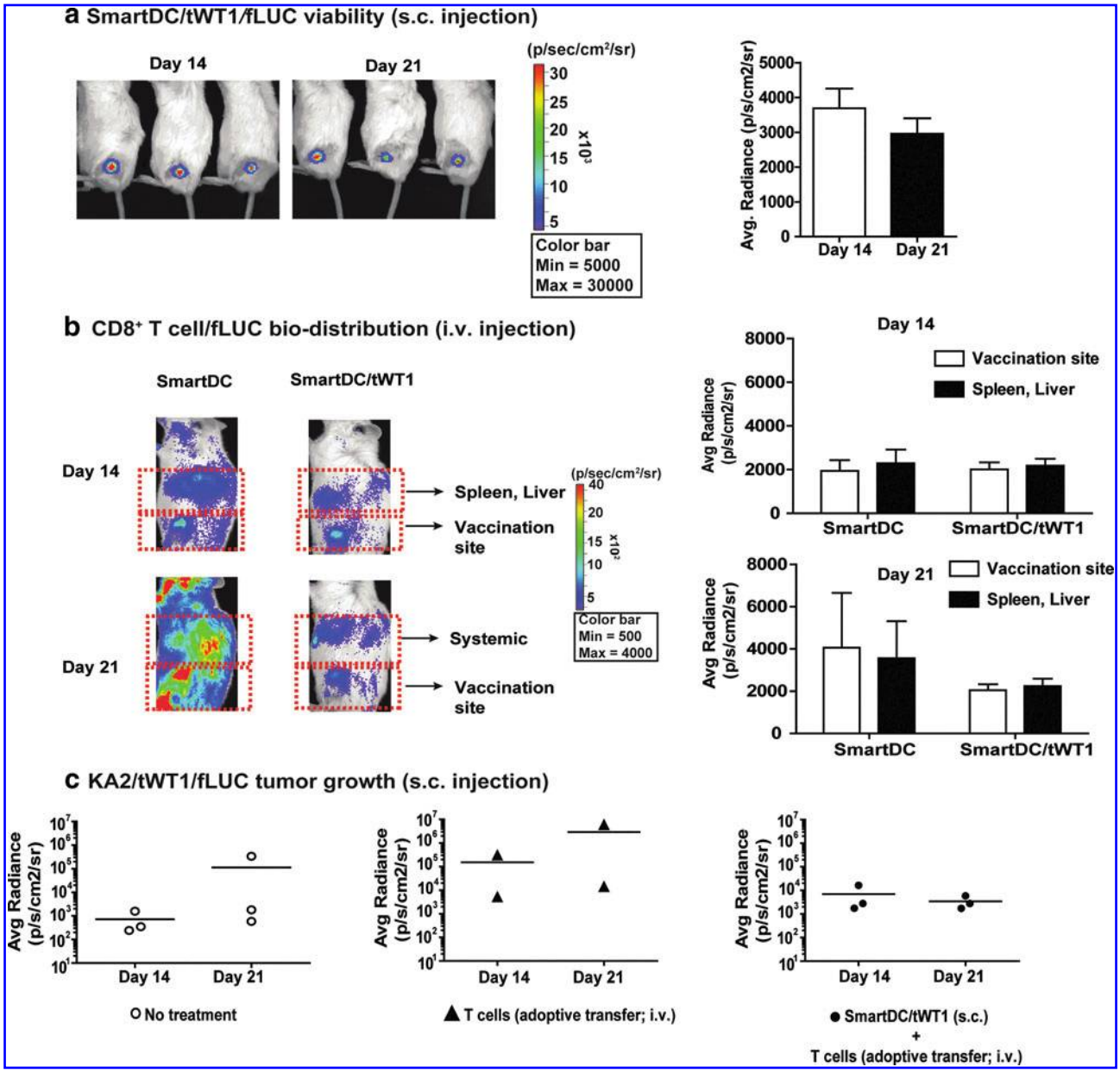

FIG. 7. Viability and potency of SmartDC/tWT1 *in vivo*. **(a)** Viability: SmartDC/tWT1/ fLUC (5×10^5 cells) were injected s.c. into the hind flanks of NRG mice and *in vivo* optical imaging analyses were performed on days 14 and 21 post injection. The reference color bar indicates high bioluminescence signals in red and low signals in blue. The bioluminescence signal emitted at the injection site was quantified and is depicted as average of radiance (n = 3). Error bars indicate standard error of mean (SEM). **(b)** T-cell biodistribution: SmartDC/tWT1 (5×10^5 cells) were injected s.c. into the hind flanks of NRG mice and $CD8^+$ T cells/fLUC were injected seven days later i.v. *In vivo* optical imaging analyses were performed 14 and 21 days after T-cell infusion for biodistribution analyses at the injection site versus systemic biodistribution (spleen and liver). The bioluminescence signals were quantified and are represented as average per group (n = 3). **(c)** Protection against KA2/WT1/ fLUC tumor growth. KA2/tWT1/fLUC (5×10^5 cells) and SmartDC/tWT1 (5×10^5 cells) were injected s.c. into the right and left hind flanks of NRG mice, respectively. Seven days later, T cells expanded *in vitro* with SmartDC/tWT1 (2×10^6 cells) were infused into mice immunized with SmartDC/tWT1. Tumor growth was monitored by optical imaging analyses 14 and 21 days after T-cell infusion. Bioluminescence signal, depicting the growth of the KA2/tWT1/fLUC, was quantified and depicted as scatter graph per group (n = 3).

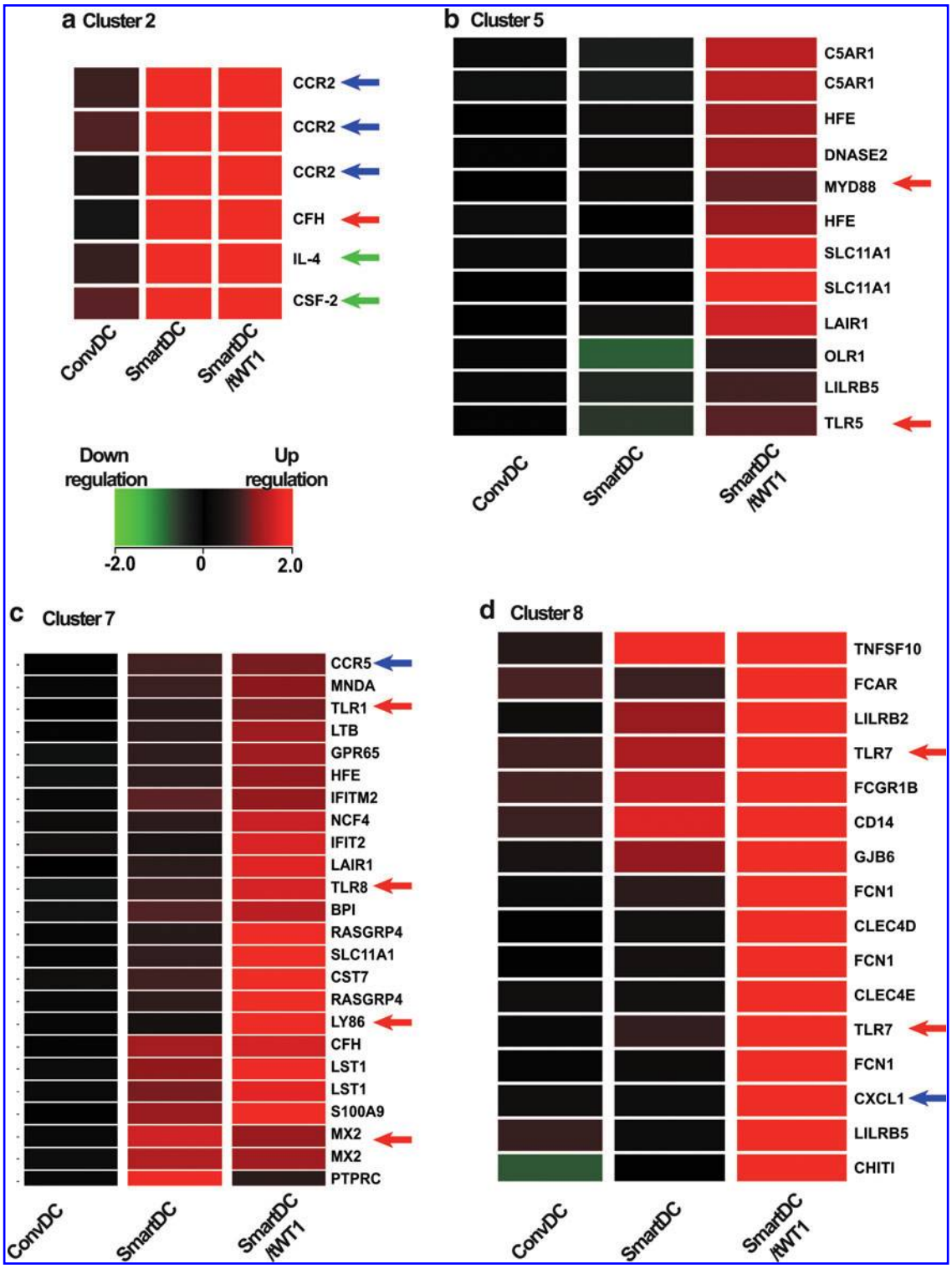

FIG. 8. Gene array analyses. Heat maps depicting clusters obtained through differential gene expression patterns of immune system processing ontology clustering by K-means. Gene expression values are given as log2 expression data. The color legend indicates the level of expression intensity: green for downregulated and red for upregulated. **(a)** Cluster 2: Identity markers upregulated in SmartDC and SmartDC/tWT1 in comparison with ConvDC. Cluster 5 **(b)**, cluster 7 **(c)**, and cluster 8 **(d)**, representing genes upregulated in SmartDC/tWT1 compared with SmartDC. Green arrows indicate the transgenic cytokines (GM-CSF and IL-4) used in DC programming; blue arrows indicate the immunophenotypic markers validated by flow cytometry, and red arrows indicate the various genes pertaining to the innate immune system that are upregulated in SmartDC/tWT1 in comparison to SmartDC and ConvDC.

Table 2. Genes Upregulated in SmartDC/tWT1 and Their Functions

Code	*Name*	*Function*
TNFSF10	TNF-related apoptosis-inducing ligand (TRAIL)	p53-dependent cell death and tumor suppression.
LILRB2 and *LILRB5*	Leukocyte immunoglobulin-like receptor, subfamily B	Binds to MHC class I molecules on antigen-presenting cells and transduces a negative signal that inhibits stimulation of an immune response. It is thought to limit autoreactivity.
FCAR	Receptor for Fc fragment of IgA	Interacts with IgA-opsonized targets and triggers several immunologic defense processes, including phagocytosis, antibody-dependent cell-mediated cytotoxicity, and stimulation of the release of inflammatory mediators.
FCGR1B	Receptor Ib for Fc fragment of IgG	After binding IgG, it interacts with the common γ chain for triggering cellular activation.
TLR7	Toll-like receptor 7	Recognizes single stranded RNA in endosomes, which is a common feature of viral genomes.
CD14	Cluster of differentiation 14	CD14 acts as a co-receptor for the detection of bacterial LPS. Soluble CD14 appears after shedding of mCD14 or is directly secreted from intracellular vesicles.
CLEC4D	C-type lectin domain family 4	Functions as an endocytic receptor. May be involved in antigen uptake at the site of infection, either for clearance of the antigen, or for processing and further presentation to T cells.
CXCL1	Chemokine (C-X-C motif) ligand 1	Plays a role in inflammation as a chemoattractant for neutrophils.
GJB6	Gap junction protein, beta 6	Specialized cell-cell contacts between almost all eukaryotic cells that provide direct intracellular communication.

Genes upregulated in SmartDC/tWT1 in comparison with SmartDC and conventional DC. The RNA microarray data was analyzed by Agilent Genespring GX11 software. Most genes are related with immune functions, such as homeostasis (TRAIL, LILRB2, LILRB5), antibody-mediated cell cytotoxicity (FCAR, FCRGR1B), innate responses (TLR7, CD14, CLEC4D), chemo-attraction (CXCL1), and cell-cell communication (GJB6).

AML patient, T-cell stimulation with SmartDC + WT1 peptide mix was superior.

In addition, we analyzed the capability of these T cells to recognize the primary leukemia blasts (marked with CFSE) using a CD107a degranulation assay. CD107a is a cytotoxicity marker, expressed on the T cells in response to the recognition of the specific target cells (Supplementary Fig. 3b). Data of this assay demonstrated that T cells expanded with SmartDC/tWT1 both from the patient and from the donor showed significantly higher degranulation than T cell expanded with SmartDC pulsed with WT1 peptides (Fig. 7d). This assay indicated that multi-antigenic stimulation resulting from endogenous processing of WT1 epitopes provides more efficient cytotoxic T cells.

In vivo *analyses of SmartDC/tWT1 immunization: viability, T-cell migration, and anti-tumor responses*

In vivo assays to validate various parameters of SmartDC/tWT1 were performed in the NRG/huCTL adoptive transfer mouse model as previously described by our group (Salguero et al., 2011). This model allows the detection of human $CD8^+$ T cell immune reactivity against the DC vaccine for 14–21 days prior to the onset of "graft-versus-mouse" responses. SmartDC/tWT1 co-expressing luciferase and administered s.c. were highly viable for 3 weeks, and thus comparable to SmartDC expressing pp65 or TRP2 (Salguero *et al.*, 2011; Pincha *et al.*, 2012) (Fig. 7a). In order to assess the ability of SmartDC/tWT1 to interact with human CTLs *in vivo*, NRG mice were preconditioned with SmartDC or SmartDC/tWT1 (5×10^5 cells) administered s.c. on the hind flanks on day -7. Mice injected with PBS served as controls. On day 0, 2×10^6 autologous $CD8^+$ T cells expressing luciferase were administered intravenously. *In vivo* bioluminescence imaging analyses were performed on days 14 and 21. On day 14, CTLs accumulated on sites where SmartDC and SmartDC/tWT1 were injected (Fig. 7b). As previously described for this model, CTLs also accumulated in the liver and spleen, which are highly fenestrated organs leading to entrapment of the infused T cells. As previously observed for SmartDC immunizations, massive T-cell expansion and biodistribution toward all parts of the mouse body was observed 21 days after adoptive T-cell transfer. Immunization with SmartDC/tWT1 resulted in lower T-cell biodistribution within the 21-day observation period.

We next sought to validate the efficacy of SmartDC/tWT1 immunization followed by adoptive T-cell transfer to protect NRG mice against challenge with a $WT1^+$ tumor; 5×10^5 KA2/tWT1 cells co-expressing luciferase were implanted s.c. on the right hind flank. Nonimmunized mice (n = 3), mice infused with T cells (n = 2), and mice immunized with SmartDC/tWT1 and infused with T cells (n = 3) were compared; 5×10^5 SmartDC/tWT1 were injected s.c. on the left hind flanks on the day of tumor challenge (on the right hind flank), and 7 days later, 2×10^6 WT1-reactive T cells that were generated *in vitro* were infused i.v. into the lateral tail vein of the immunized mice. Tumor growth was monitored noninvasively by optical imaging analyses. Within the first 21 days after challenge, nontreated mice or mice infused with T cells showed tumor growth, whereas mice immunized

with SmartDC/tWT1 and infused with T cells showed an arrest in tumor development (Fig. 7c). Since the human T cells infused i.v. in the mice eventually react nonspecifically to mouse antigens and cause graft-versus-host disease, this model can only be explored for determining potency *in vivo* during a short observation period.

Gene expression patterns of SmartDC and SmartDC/tWT1

Analyses of SmartDC/tWT1 *in vitro* and *in vivo* showed the expected functions, namely high viability along with immune stimulation against WT1. Nevertheless, since WT1 is a complex transcription factor with several regulatory functions, we evaluated possible unintended effects of expression of truncated WT1 on the transcriptional regulation of SmartDC. We used gene array analyses to compare the RNA expression in ConvDC with SmartDC and SmartDC/tWT1. In order to obtain homogeneous cells with high DC viability and purity (>80% $HLADR^+/CD86^+$), independent cultures (n=6) were maintained for 14 days *in vitro* prior to harvest and RNA purification. To further delineate the expression data matrix, we applied K-means clustering to obtain gene ontology groups associated with a common gene expression profile (Fig. 8). The microarray system was used initially to confirm identity and potency markers. As expected, GM-CSF (CSF-2) and IL-4 were highly upregulated in SmartDC/tWT1 and SmartDC (Fig. 8a). Transcripts encoding chemokine receptors previously characterized by FACS (CCR2, CCR5) (Fig. 8a and c) were also upregulated. Three clusters representing immune regulatory genes specifically upregulated in SmartDC and/or SmartDC/tWT1 were further analyzed (Fig. 8c and d). Remarkably, several of the mRNAs upregulated in SmartDC and/or SmartDC/tWT1 were involved with innate immune responses, such as toll-like receptors (TLR 1, 5, 7, 8), a TLR adaptor (MyD88), antiviral proteins (MX2, LTB), antibacterial proteins (SLC11A1), and a complement component (C5AR1). Cluster 8 (Fig. 8d, Table 2) showed the transcripts that were expressed at higher levels in SmartDC/tWT1 compared with ConvDC or SmartDC. TRAIL, which is a protein constitutively expressed in natural killer (NK) cells and that can be upregulated in NK and T cells, was highly expressed in SmartDC/tWT1. TRAIL can induce apoptotic cell death in transformed cells and is also involved with maintenance of immunologic homeostasis (such as modulating acute graft-versus-host disease). It was shown that DC genetically modified with adenoviral vectors for TRAIL expression protected mice from acute GVHD and leukemia relapse (Sato *et al.,* 2005). Moreover, two forms of the leukocyte immunoglobulin-like receptors (LILRB2 and LILRB5) were highly expressed in SmartDC/tWT1 indicating that class I responses in these cells could be potentially modulated to avoid overt reactivity. Furthermore, SmartDC/tWT1 also seem to highly express receptors for immunoglubulins (IgA and IgG), which could potentially result into cell activation by antibodies. Transcripts of products involved with innate immune responses upregulated in SmartDC/tWT1 were TLR7, CD14, and CXCL1. Remarkably, the gene array analyses also showed upregulation of the mRNA encoding for the gap junction protein beta 6 in SmartDC/tWT1, indicating the possibility of intracellular communication for exchange of antigens and cytokines. This would potentially enhance the function of SmartDC/tWT1 as it has been demonstrated that gap junction–mediated communication between DC may be, in fact, required for effective activation (Matsue *et al.,* 2006). Thus, the microarray analyses indicated that co-expression of tWT1 in SmartDC/tWT1 served to enhance multivalent immune functions.

Discussion

Several clinical trials exploring antigenic WT1 peptides for immunization of AML patients showed immunogenic and anti-leukemia responses. However, immunological responses and clinical outcomes reported to date were quite variable and several doses of vaccinations were required for sustained clinical outcome (Rezvani *et al.,* 2008; Keilholz *et al.,* 2009). Incidentally, repeated vaccinations with a class I WT1 peptide ($WT1_{126–134}$) was reported to actually lead to worrisome deletion of high avidity and functional T cells from the patients (Kuball *et al.,* 2011; Rezvani *et al.,* 2011). This indicates that immune surveillance against WT1 might demand a rather broad repertoire of long-lasting adaptive immune responses and that immune-dominant epitopes suboptimally presented by APCs might promote anergy or T-cell exhaustion. Thus, optimized endogenous presentation of multi-antigenic WT1 epitopes through innate, class I and class II pathways may have to be considered to optimize the immunotherapeutic effects of WT1. Recently, DC transfected with WT1 RNA allowing several WT1 antigenic epitopes to be presented have demonstrated successful clinical responses in phase I clinical trial (Van Tendeloo *et al.,* 2010), but the practicality of large-scale production remains an issue.

As an alternative to *ex vivo* generation of DC using conventional methods (i.e., incubation of monocytes with cytokines for several days followed by antigenic pulsing or RNA transfection), we demonstrated that a tricistronic non-replicating and self-inactivating lentiviral vector–expressing cytokines and a melanoma antigen (tyrosine-related protein 2, TRP2) directly induced the differentiation of monocytes into highly viable DC ("SmartDC") capable of endogenously processing the melanoma antigen TRP2 (Pincha *et al.,* 2012) or the pp65 cytomegalovirus protein (Koya *et al.,* 2007; Pincha *et al.,* 2011, 2012; Salguero *et al.,* 2011). In mouse and in *in vitro* human models, "SmartDC" were shown to be superior to ConvDC in viability, biodistribution, and antigen-specific immune responses (Koya *et al.,* 2007; Pincha *et al.,* 2011, 2012; Salguero *et al.,* 2011). $NOD.Rag^{-/-}IL2r\gamma c^{-/-}$ mice injected subcutaneously with human SmartDC co-expressing pp65 prior to adoptive T-cell transfer showed a dramatic enhancement of the expansion and immune reactivity of pp65-specific $CD8^+$ central memory T cells (Salguero *et al.,* 2011).

Here, we tested the generation of SmartDC expressing a truncated form of WT1. It was previously reported that overexpression of the truncated WT1, which lacks the zinc finger DNA-binding domain, by retroviral gene modification of $CD34^+$ hematopoietic progenitors resulted in a reduced myelogenous clonogenic growth and stimulated myeloid differentiation (Svensson *et al.,* 2005). Agreeing to these results, persistent expression of tWT1 in DC programmed with the tricistronic LV-G242W vector did not compromise their

viability or differentiation. Endogenous sustained production of cytokines (GM-CSF, IL-4, IL-6, and TNF-a), chemokines (IL-8, MCP-1), and chemokine receptors (CCR2, CCR5) were also observed for SmartDC expressing the melanoma antigen TRP2 (Pincha *et al.*, 2012). Immunization of immune competent C57BL/6 mice with the mouse-homologous SmartDC/TRP2 stimulated cytotoxic responses against $TRP2^+$ B16 melanoma cells and occasionally vitiligo and alopecia (TRP2 is expressed in melanocytes present in the hair follicles) (Pincha *et al.*, 2012). Nevertheless, mice did not show any signs of progressive generalized autoimmunity or toxicity. For SmartDC/tWT1, since it was recently shown that patients with trisomy 8 with myelodypsplastic syndrome (MDS) show detectable levels of $CD8^+$ T-cell responses directed against WT1 in hematopoieitic progenitor cells, a hypothetical concern would be that the potent anti-WT1 immune response generated by SmartDC/tWT1 could lead to reactivity against hematopoietic progenitor cells and myelosuppression (Sloand *et al.*, 2011). This biosafety concern remains to be evaluated in immune-competent mouse models or in immune-deficient mice reconstituted with human hematopoietic stem cells.

Notably, gene array analyses of mRNA transcripts present in SmartDC/tWT1 indicated that the truncated form of WT1 might exert immune regulatory functions such as upregulation of innate responses, homeostatic responses, immunity against bacteria, and viruses and antibody-dependent cell-mediated cytotoxicity. It is known that viral infections can substantially alter the gene expression pattern of dendritic cells (Zilliox *et al.*, 2006). We did not expect any late effects due to lentiviral vector transduction, as SmartDC/tWT1 and SmartDC were analyzed by gene array 2 weeks after viral transduction. Therefore, some of these gene modulations appear to be caused by overexpression of tWT1. To our knowledge, WT1 expression in genetically manipulated human DC lasting for several weeks has not been reported. It is tempting to speculate that the amino-terminus of WT1 may stimulate DC differentiation and/or activation.

Several prior reports described the complex requirements for *in vitro* generation of $CD8^+$ T cells reactive against WT1 (Ho *et al.*, 2006; Wolfl *et al.*, 2007). In general, these lengthy protocols included several rounds of stimulation of enriched $CD8^+$ T cells in the presence of multiple cytokines and antigenic peptides. Using SmartDC/tWT1, two rounds of *in vitro* stimulation were required to observe initial expansion of autologous reactive $CD8^+$ T cells, and this was further increased by a third stimulation. Our results were highly reproducible in experiments performed with cells from different donors (Table 1). In our patient–donor model, the patient carried a very aggressive leukemia oncogene, FLT3-ITD. These patients are at very high risk of leukemia recurrence, and therefore the standard of care commonly includes hematopoietic stem cell transplantation (HSCT) and adoptive T-cell transfer (Schlenk *et al.*, 2008; Bacher *et al.*, 2009). Studies from our group with diagnostic and remission samples obtained from FLT3-ITD patients showed a deregulated dendropoiesis, accumulation of dendritic cell precursors, and aberrant expression of inflammatory cytokines (Rickmann *et al.*, 2011). Notably, FLT3-ITD occurrence has been correlated with WT1 overexpression (Spassov *et al.*, 2011). Therefore, WT1 could be a particularly applicable candidate antigen for immunotherapy of this aggressive type of leukemia in the context of lymphodepletion followed by stem cell transplantation.

Despite several recent clinical advances, the field of "immunogene-therapy" using lentiviral vectors is still just beginning (Pincha *et al.*, 2010). T cells engineered with lentiviral vectors to express chimeric antigen receptors (CARs) have been used clinically with tremendous success for lymphoma immunotherapy (Kalos *et al.*, 2011; Porter *et al.*, 2011), and hematopoietic stem cells from patients carrying genetic abnormalities have been "corrected" with lentiviral vectors (Cartier *et al.*, 2009). These clinical trials have so far not shown any adverse effects due to lentiviral transduction, and the lentiviral integration pattern seems to be rather benign (Biffi *et al.*, 2011). Large-scale manufacture of lentiviral vectors for clinical use (Merten *et al.*, 2011) is now available, and a method for GMP-compliant production of cryopreserved SmartDC has been described by our group (Pincha *et al.*, 2012). Thus, based on the simplicity of production and taking into account their broad homeostatic and antigenic properties, SmartDC/tWT1 could represent a realistic new platform for effective active immuno-regenerative therapy against high-risk AML and additional neoplasms displaying WT1 upregulation (such as lymphoma, melanoma, lung, and breast cancers).

Acknowledgments

We would like to thank Prof. Vigo van Tendeloo (Univ. Antwerp) for technical assistance and discussions and Prof. Schwinzer for technical assistance in setting up the thymidine incorporation assays. We thank Dr. Adan Jirmo and Dr. Verena Schlaphoff for their help and discussions with CFSE-based cytotoxicity assays. We thank the leukemia patients and healthy volunteers who kindly provided us with peripheral blood and leukapheresis samples, and the clinical staff (Prof. Dr. Juergen Krauter, Dr. Kathrin Stamer, Dr. Anke Breithaupt, Dr. Pauline Lübben, Dr. Kamal Haytham, and Dr. Lillia Goudeva) for all the coordinations. This work was supported by funds from the German José Carreras Leukemia Foundation (R09/05), Excellence Cluster Rebirth (DFG), SFB738 and Deutsche Krebshilfe (to R.S.). B.S. received a PhD fellowship from the Excellence Cluster Rebirth (DFG).

Author Disclosure Statement

The authors have no conflicts of interest to disclose.

References

Bacher, U., Haferlach, C., Schnittger, S., *et al.* (2009). Interactive diagnostics in the indication to allogeneic SCT in AML. Bone Marrow Transplant 43, 745–56.

Betts, M.R., Brenchley, J.M., Price, D.A., *et al.* (2003). Sensitive and viable identification of antigen-specific CD8+ T cells by a flow cytometric assay for degranulation. J. Immunol. Methods 281, 65–78.

Biffi, A., Bartolomae, C.C., Cesana, D., *et al.* (2011). Lentiviral vector common integration sites in preclinical models and a clinical trial reflect a benign integration bias and not oncogenic selection. Blood 117, 5332–9.

Britten, C.M., Meyer, R.G., Kreer, T., *et al.* (2002). The use of HLA-A*0201-transfected K562 as standard antigen-presenting

cells for CD8(+) T lymphocytes in IFN-gamma ELISPOT assays. J. Immunol. Methods 259, 95–110.
Cartier, N., Hacein-Bey-Abina, S., Bartholomae, C.C., *et al.* (2009). Hematopoietic stem cell gene therapy with a lentiviral vector in X-linked adrenoleukodystrophy. Science 326, 818–23.
Case S.S., Price, M.A., Jordan, C.T., *et al.* (1999). Stable transduction of quiescent CD34(+)CD38(-) human hematopoietic cells by HIV-1-based lentiviral vectors. Proc. Natl. Acad. Sci. U.S.A 96, 2988–93.
Cavalieri, S., Cazzaniga, S., Geuna, M., *et al.* (2003). Human T lymphocytes transduced by lentiviral vectors in the absence of TCR activation maintain an intact immune competence. Blood 102, 497–505.
Cilloni, D., Renneville, A., Hermitte, F., *et al.* (2009). Real-time quantitative polymerase chain reaction detection of minimal residual disease by standardized WT1 assay to enhance risk stratification in acute myeloid leukemia: a European LeukemiaNet study. J. Clin. Oncol. 27, 5195–201.
Gupta, V., Tallman, M.S., and Weisdorf, D.J. (2011). Allogeneic hematopoietic cell transplantation for adults with acute myeloid leukemia: myths, controversies, and unknowns. Blood 117, 2307–18.
Ho, W.Y., Nguyen, H.N., Wolfl, M., *et al.* (2006). In vitro methods for generating CD8+ T-cell clones for immunotherapy from the naive repertoire. J. Immunol. Methods 310, 40–52.
Jedema, I., Van Der Werff, N.M., Barge, R.M., *et al.* (2004). New CFSE-based assay to determine susceptibility to lysis by cytotoxic T cells of leukemic precursor cells within a heterogeneous target cell population. Blood 103, 2677–82.
Kalos, M., Levine, B.L., Porter D.L., *et al.* (2011). T cells with chimeric antigen receptors have potent antitumor effects and can establish memory in patients with advanced leukemia. Sci. Transl. Med. 3, 95ra73.
Keilholz, U., Letsch, A., Busse, A., *et al.* (2009). A clinical and immunologic phase 2 trial of Wilms tumor gene product 1 (WT1) peptide vaccination in patients with AML and MDS. Blood 113, 6541–8.
Koya, R.C., Kimura, T., Ribas, A., *et al.* (2007). Lentiviral vector-mediated autonomous differentiation of mouse bone marrow cells into immunologically potent dendritic cell vaccines. Mol. Ther. 15, 971–80.
Koya, R.C., Weber, J.S., Kasahara, N., *et al.* (2004). Making dendritic cells from the inside out: lentiviral vector-mediated gene delivery of granulocyte-macrophage colony-stimulating factor and interleukin 4 into CD14+ monocytes generates dendritic cells in vitro. Hum. Gene Ther. 15, 733–48.
Kuball, J., De Boer, K., Wagner, E., *et al.* (2011). Pitfalls of vaccinations with WT1-, Proteinase3- and MUC1-derived peptides in combination with MontanideISA51 and CpG7909. Cancer Immunol. Immunother. 60, 161–71.
Maslak, P.G., Dao, T., Krug, L.M., *et al.* (2010). Vaccination with synthetic analog peptides derived from WT1 oncoprotein induces T-cell responses in patients with complete remission from acute myeloid leukemia. Blood 116, 171–9.
Matsue, H., Yao, J., Matsue, K., *et al.* (2006). Gap junction-mediated intercellular communication between dendritic cells (DCs) is required for effective activation of DCs. J. Immunol. 176, 181–90.
Merten, O.W., Charrier, S., Laroudie, N., *et al.* (2011). Large-scale manufacture and characterization of a lentiviral vector produced for clinical ex vivo gene therapy application. Hum. Gene Ther. 22, 343–56.
Pincha, M., Sundarasetty, B.S., and Stripecke, R. (2010). Lentiviral vectors for immunization: an inflammatory field. Expert Rev. Vaccines 9, 309–21.
Pincha, M., Salguero, G., Wedekind, D., *et al.* (2011). Lentiviral vectors for induction of self-differentiation and conditional ablation of dendritic cells. Gene Ther. 18, 750–64.
Pincha, M., Sundarasetty, B.S., Salguero, G., *et al.* (2012). Identity, potency, in vivo viability, and scaling up production of lentiviral vector-induced dendritic cells for melanoma immunotherapy. Hum. Gene Ther. Methods 23, 38–55.
Porter, D.L. (2011). Allogeneic immunotherapy to optimize the graft-versus-tumor effect: concepts and controversies. Hematology Am. Soc. Hematol. Educ. Program 2011, 292–8.
Porter, D.L., Levine, B.L., Kalos, M., *et al.* (2011). Chimeric antigen receptor-modified T cells in chronic lymphoid leukemia. N. Engl. J. Med. 365, 725–33.
Pospori, C., Xue, S.A., Holler, A., *et al.* (2011). Specificity for the tumor-associated self-antigen WT1 drives the development of fully functional memory T cells in the absence of vaccination. Blood 117, 6813–24.
Rezvani, K., Yong, A.S., Mielke, S., *et al.* (2008). Leukemia-associated antigen-specific T-cell responses following combined PR1 and WT1 peptide vaccination in patients with myeloid malignancies. Blood 111, 236–42.
Rezvani, K., Yong, A.S., Mielke, S., *et al.* (2011). Repeated PR1 and WT1 peptide vaccination in Montanide-adjuvant fails to induce sustained high-avidity, epitope-specific CD8+ T cells in myeloid malignancies. Haematologica 96, 432–40.
Rickmann, M., Krauter, J., Stamer, K., *et al.* (2011). Elevated frequencies of leukemic myeloid and plasmacytoid dendritic cells in acute myeloid leukemia with the FLT3 internal tandem duplication. Ann. Hematol. 90, 1047–58.
Salguero, G., Sundarasetty, B.S., Borchers, S., *et al.* (2011). Preconditioning therapy with lentiviral vector-programmed dendritic cells accelerates the homeostatic expansion of antigen-reactive human T cells in NOD.Rag1−/−.IL-2rgammac−/− mice. Hum. Gene Ther. 22, 1209–24.
Sato, K., Nakaoka, T., Yamashita, N., *et al.* (2005). TRAIL-transduced dendritic cells protect mice from acute graft-versus-host disease and leukemia relapse. J. Immunol. 174, 4025–33.
Scheibenbogen, C., Letsch, A., Thiel, E., *et al.* (2002). CD8 T-cell responses to Wilms tumor gene product WT1 and proteinase 3 in patients with acute myeloid leukemia. Blood 100, 2132–7.
Schlenk, R.F., Dohner, K., Krauter, J., *et al.* (2008). Mutations and treatment outcome in cytogenetically normal acute myeloid leukemia. N. Engl. J. Med. 358, 1909–18.
Sloand, E.M., Melenhorst, J.J., Tucker, Z.C., *et al.* (2011). T-cell immune responses to Wilms tumor 1 protein in myelodysplasia responsive to immunosuppressive therapy. Blood 117, 2691–9.
Spassov, B.V., Stoimenov, A.S., Balatzenko, G.N., *et al.* (2011). Wilms' tumor protein and FLT3-internal tandem duplication expression in patients with de novo acute myeloid leukemia. Hematology 16, 37–42.
Stripecke, R. (2009). Lentiviral vector-mediated genetic programming of mouse and human dendritic cells. Methods Mol. Biol. 506, 139–58.
Sugiyama, H. (2010). WT1 (Wilms' tumor gene 1): biology and cancer immunotherapy. Jpn. J. Clin. Oncol. 40, 377–87.
Svensson, E., Eriksson, H., Gekas, C., *et al.* (2005). DNA-binding dependent and independent functions of WT1 protein during human hematopoiesis. Exp. Cell Res. 308, 211–21.

Van Tendeloo, V.F., Van De Velde, A., Van Driessche, A., *et al.* (2010). Induction of complete and molecular remissions in acute myeloid leukemia by Wilms' tumor 1 antigen-targeted dendritic cell vaccination. Proc. Natl. Acad. Sci. U.S.A. 107, 13824–9.

Weber, G., Karbach, J., Kuci, S., *et al.* (2009). WT1 peptide-specific T cells generated from peripheral blood of healthy donors: possible implications for adoptive immunotherapy after allogeneic stem cell transplantation. Leukemia 23, 1634–42.

Wolfl, M., Kuball, J., Ho, W.Y., *et al.* (2007). Activation-induced expression of CD137 permits detection, isolation, and expansion of the full repertoire of CD8+ T cells responding to antigen without requiring knowledge of epitope specificities. Blood 110, 201–10.

Zilliox, M.J., Parmigiani, G., and Griffin, D.E. (2006). Gene expression patterns in dendritic cells infected with measles virus compared with other pathogens. Proc. Natl. Acad. Sci. U.S.A. 103, 3363–8.

Address correspondence to:
Prof. Renata Stripecke
Department of Hematology, Hemostasis
Oncology and Stem Cell Transplantation
Lymphatic Cell Therapy Laboratory
Hannover Medical School
Carl-Neuberg-Strasse 1
OE6860 – J11/HBZ Room 6100
D-30625 Hannover
Germany

E-mail: stripecke.renata@mh-hannover.de

Received for publication June 21, 2012;

accepted after revision December 14, 2012.
Published online: January 10, 2013.